

# Endogenous SNAP-25 Regulates Native Voltage-gated Calcium Channels in Glutamatergic Neurons\*

Received for publication, May 18, 2010. Published, JBC Papers in Press, June 3, 2010, DOI 10.1074/jbc.M110.145813

Steven B. Condliffe<sup>†1</sup>, Irene Corradini<sup>‡</sup>, Davide Pozzi<sup>‡2</sup>, Claudia Verderio<sup>‡</sup>, and Michela Matteoli<sup>‡§</sup>

From the <sup>†</sup>Department of Medical Pharmacology and Consiglio Nazionale delle Ricerche Institute of Neuroscience, University of Milano, Via Vanvitelli 32, 20129 Milano and the <sup>§</sup>IRCCS Fondazione Don Gnocchi, 20122 Milano, Italy

In addition to its primary role as a fundamental component of the SNARE complex, SNAP-25 also modulates voltage-gated calcium channels (VGCCs) in various overexpression systems. Although these studies suggest a potential negative regulatory role of SNAP-25 on VGCC activity, the effects of endogenous SNAP-25 on native VGCC function in neurons are unclear. In the present study, we investigated the VGCC properties of cultured glutamatergic and GABAergic rat hippocampal neurons. Glutamatergic currents were dominated by P/Q-type channels, whereas GABAergic cells had a dominant L-type component. Also, glutamatergic VGCC current densities were significantly lower with enhanced inactivation rates and shifts in the voltage dependence of activation and inactivation curves compared with GABAergic cells. Silencing endogenous SNAP-25 in glutamatergic neurons did not alter P/Q-type channel expression or localization but led to increased VGCC current density without changes in the VGCC subtype proportions. Isolation of the P/Q-type component indicated that increased current in the absence of SNAP-25 was correlated with a large depolarizing shift in the voltage dependence of inactivation. Overexpressing SNAP-25 in GABAergic neurons reduced current density without affecting the VGCC subtype proportion. Accordingly, VGCC current densities in glutamatergic neurons from *Snap-25*<sup>+/-</sup> mice were significantly elevated compared with wild type glutamatergic neurons. Overall, this study demonstrates that endogenous SNAP-25 negatively regulates native VGCCs in glutamatergic neurons which could have important implications for neurological diseases associated with altered SNAP-25 expression.

The primary role of SNAP-25<sup>3</sup> is as a fundamental component of the SNARE complex responsible for vesicle fusion (1). In addition to mediating exocytosis by binding to other SNARE

proteins, SNAP-25 has also been shown to interact with and modulate a variety of other proteins involved in diverse functions (2–4). Important among these interactions are the voltage-gated calcium channels (VGCCs), where SNAP-25 overexpression generally results in a negative modulation of VGCC function (5). However, the majority of the studies describing this regulatory role have been performed by overexpressing SNAP-25 and VGCCs in heterologous systems (6, 7). Although Pozzi *et al.* (8) recently demonstrated that SNAP-25 negatively modulates native VGCC function in neurons, the effect was still observed while overexpressing exogenous SNAP-25. It is possible that these effects on VGCC function could result from nonspecific interactions forced via the molecular arrangement of the proteins in the plasma membrane as a consequence of overexpression.

The objective of the present study was to investigate whether endogenous SNAP-25 is effective in regulating native VGCC function in neurons. In particular, if SNAP-25 is physiologically involved in regulating VGCC function, then the reduction of endogenous SNAP-25 expression in neurons would remove a regulatory “brake” on calcium channel function, leading to alterations in VGCC properties. This would not only reveal the physiological role of SNAP-25 in controlling native VGCC function but would also have important implications for brain pathologies where the levels of SNAP-25 are altered (9–11).

To address this issue, we measured native VGCC function in cultured hippocampal glutamatergic and GABAergic neurons. Our results demonstrate that these different neuronal cell types exhibit distinct VGCC current properties with diverse VGCC subtype expression profiles. Moreover, silencing of endogenous SNAP-25 in glutamatergic neurons enhances VGCC current density with significant increases in inactivation rates and a depolarizing shift in the voltage dependence of inactivation. Importantly, we also found similar increases in VGCC function in glutamatergic neurons from SNAP-25 heterozygous mice. These results demonstrate that levels of endogenous SNAP-25 negatively modulate native VGCC function, which could have important consequences for brain diseases characterized by a reduced SNAP-25 expression.

## EXPERIMENTAL PROCEDURES

**Hippocampal Neuronal Cultures**—Primary cultures of rat or mouse hippocampal neurons were prepared from the hippocampi of 18-day-old fetuses as previously described (12) and plated at low density on glass coverslips. Neurons were transfected at 5–6 DIV using the calcium phosphate precipitation method. Silencing of SNAP-25 was achieved via transfection of

\* This work was supported by the European Union 7th Framework Program Grant HEALTH F2-2009-241498 (EUROSPIN Project), EUSynapse Integrated Project, Cariplo 2008.2338, Cariplo 2006.0948, and Compagnia di S. Paolo Program 2005.1964 (to M. M.).

<sup>1</sup> To whom correspondence should be sent at the present address: Dept. of Physiology, University of Otago, P. O. Box 913, Dunedin 9054, New Zealand. Tel.: 64-3-479-7338; Fax: 64-3-479-5419; E-mail: steven.condliffe@otago.ac.nz.

<sup>2</sup> Present address: Italian Institute of Neuroscience, Via Morego 30, 16163 Genoa, Italy.

<sup>3</sup> The abbreviations used are: SNAP-25, synaptosomal-associated protein of 25 kDa; DIV, days *in vitro*; GABA,  $\gamma$ -aminobutyric acid; GFP, green fluorescent protein; *I-V*, current-voltage; RT, reverse transcription; siRNA, small interfering RNA; SNARE, soluble *N*-ethylmaleimide-sensitive factor attachment protein receptors; VGAT, vesicular GABA transporter; VGCC, voltage-gated calcium channel; VGlut, vesicular glutamate transporter.

a pSUPER construct (13). A nonspecific siRNA duplex of the same nucleotides but in an irregular sequence (scrambled iSNAP-25 siRNA) was prepared using oligonucleotides 5'-GAT-CCCCGAGGAGTTATGCGATAGTATTCAAGAGAATG-ATAGCGTATTGAGGAGTTTTTGGAAA-3' and 5'-AGCT-TTTCCAAAACTCCTCAATACGCTATCATTCTCTTG-AATACTATCGCATAACTCCTCGGG-3' that were annealed and ligated into the pSuper vector as described previously (13).

**Electrophysiology**—Whole cell VGCC currents were recorded from 9–13-DIV neurons as described previously (8). Briefly, neurons were bathed in an external solution containing 115 mM NaCl, 4 mM KCl, 10 mM BaCl<sub>2</sub>, 1 mM MgCl<sub>2</sub>, 10 mM tetraethylammonium chloride, 10 mM glucose, 10 mM HEPES, and 1 μM tetrodotoxin, pH 7.4) where transfection of individual neurons was confirmed via positive fluorescence using an Axiovert 200 inverted fluorescence microscope (Zeiss). Patch pipettes with resistances measuring 2–4 MΩ were filled with internal recording solution (120 mM CsMeSO<sub>4</sub>, 4 mM MgCl<sub>2</sub>, 10 mM EGTA, 10 mM HEPES, 4 mM MgATP, and 3 mM Tris-GTP, pH 7.2, with CsOH), and peak whole cell Ba<sup>2+</sup> currents were measured using an Axopatch 200B amplifier (Axon Instruments) interfaced to a PC via a Digidata 1320 (Axon Instruments). For experiments measuring blocker sensitivity, VGCC blockers were perfused via a gravity-driven perfusion system into a small volume (300 μl) perfusion chamber (Warner Instruments) enabling a rapid and complete bath exchange. Data were acquired at 5 kHz with leak and capacitive transients subtracted on-line with a P/4 protocol using pClamp 8.0 software. Series resistance was routinely compensated at 60–75%, and access resistance was monitored continually during the experiments such that cells with uncompensated voltage errors >5 mV were excluded from analysis. *I-V*, activation, and inactivation curves were fit with modified Boltzmann functions. Inactivation kinetics were determined from a double-exponential fit of the current decay in response to a 1-s depolarization from –80 to 0 mV. Unless indicated otherwise, data are expressed as the mean ± S.E. of *n* experiments with statistical significance determined using a paired *t* test at the *p* level indicated.

**Single-cell RT-PCR**—Single-cell RT-PCR experiments were based on methodology described previously (14). For single-cell RT-PCR electrophysiological recordings, patch pipettes were fabricated from capillaries that were pretreated by heating at 200 °C overnight and pulled to resistances of 1.5–2 MΩ when filled with an autoclaved RT-PCR internal solution (135 mM CsCl<sub>2</sub>, 4 mM MgCl<sub>2</sub>, 5 mM EGTA, 5 mM HEPES, pH 7.2, with CsOH). After electrophysiological recordings, neuronal cytoplasm was aspirated into the recording pipette, and pipette contents were then expelled into an RNase-free 0.5-ml microcentrifuge tube containing hexamer primers and dNTPs followed by RT using the Superscript III RT-PCR kit (Invitrogen) according to the manufacturer's instructions. All reactions included a positive control using purified adult rat hippocampal RNA and a negative control of a mock harvest. Control reactions performed in the absence of Superscript III reverse transcriptase excluded the possibility that genomic DNA was being amplified in subsequent PCRs. A first round of amplification using 5–10 μl of RT cDNA was performed with 35–40 cycles of

PCR using Platinum *Taq* polymerase (Invitrogen) or RedTaq (Sigma), and gene-specific primers for VGAT (forward primer, 5'-CAC GTC GCA GAT CTT CCT GC-3'; reverse primer, 5'-GT CTT CAC GCT GCT CAT GGC-3' sequence) and VGlut (forward primer, 5'-CAT CTC CTT CCT GGT CCT GG-3'; reverse primer, 5'-CTG CCT CAG GCT TAA GAT GC-3'). A second round of PCR (25 cycles) was then performed using 1–5 μl of the first-round PCR with the same reverse primers but a nested forward primer for both VGAT (nested forward primer, 5'-CAG CCC AGC GAA TTC CAC TG-3') and VGlut (nested forward primer, 5'-GAA CCA CTT GGA CAT CGC CC-3') to generate 347- and 523-bp products, respectively. Reaction products were then identified on an ethidium bromide 2% agarose gel.

**Cell Fractionation**—Mouse brain fractionation was carried out by means of differential centrifugation as described previously (15, 16). Briefly, cerebral cortices dissected from mouse brains were homogenized in homogenization buffer (10 mM Hepes, pH 7.4, containing 0.3 M sucrose and proteases inhibitors); the total homogenate was centrifuged for 10 min at 800 × *g*, and the postnuclear supernatant (S1) was collected and centrifuged 1 h at 196,000 × *g* to yield a high speed supernatant corresponding to the cytosol and a pellet enriched in membrane-bound organelles.

**Immunocytochemistry**—Hippocampal cultures were fixed and stained as described (17). The images were acquired using an MRC-1024 confocal microscope (Bio-Rad) equipped with LaserSharp 3.2 software with fixed parameters. The average intensity of stained neurons in the somatodendritic regions was measured by ImageJ-1.4.3.67 software (National Institutes of Health).

**Reagents and Antibodies**—Polyclonal antibodies against rat Ca<sub>v</sub>1.2 (L-type) and Ca<sub>v</sub>2.1 (P/Q-type) channels were kind gifts of Dr. W. A. Catterall (University of Washington, L- and P/Q-types) and Dr. P. Rosa (Consiglio Nazionale delle Ricerche, Milano, P/Q-type) used for immunocytochemistry as previously described (18–20). Antibodies to Ca<sub>v</sub>2.1 P/Q-type channels and antibodies to the α2δ2 auxiliary subunit of VGCCs were from Alomone Laboratories (Jerusalem, Israel) and BD Biosciences, respectively, and were used for Western blotting. Monoclonal anti-SNAP-25 antibodies (SMI 81) were purchased from Sternberger Monoclonals (Baltimore, MD). Antibodies against VGlut1 were from Synaptic Systems (Goettingen, Germany). Human sera from patients affected by stiff man syndrome and specifically recognizing glutamic acid decarboxylase were provided by Dr. M. Solimena (Dresden, Germany). The antibodies to Hsp70 (BRM-22 clone) and syntaxin (HPC-1 clone) were from Sigma (Milan). Anti-NR2A was from Zymed Laboratories Inc. (San Francisco, CA). Anti-NR1 was from Synaptic Systems. Anti-Na/K-ATPase was a kind gift from Dr. G. Pietrini (University of Milan) (21). Secondary antibodies were from Jackson ImmunoResearch Laboratories (Cy-5) and from Invitrogen (Alexa Fluor 488 and Alexa Fluor 568). Fixed cells were detergent-permeabilized, incubated with primary and secondary antibodies, and mounted in Mowiol mounting medium. After fixation and staining, images were acquired using a Bio-Rad MRC-1024 confocal microscope equipped with LaserSharp 3.2 software.

## Neuronal Calcium Channel Regulation by SNAP-25

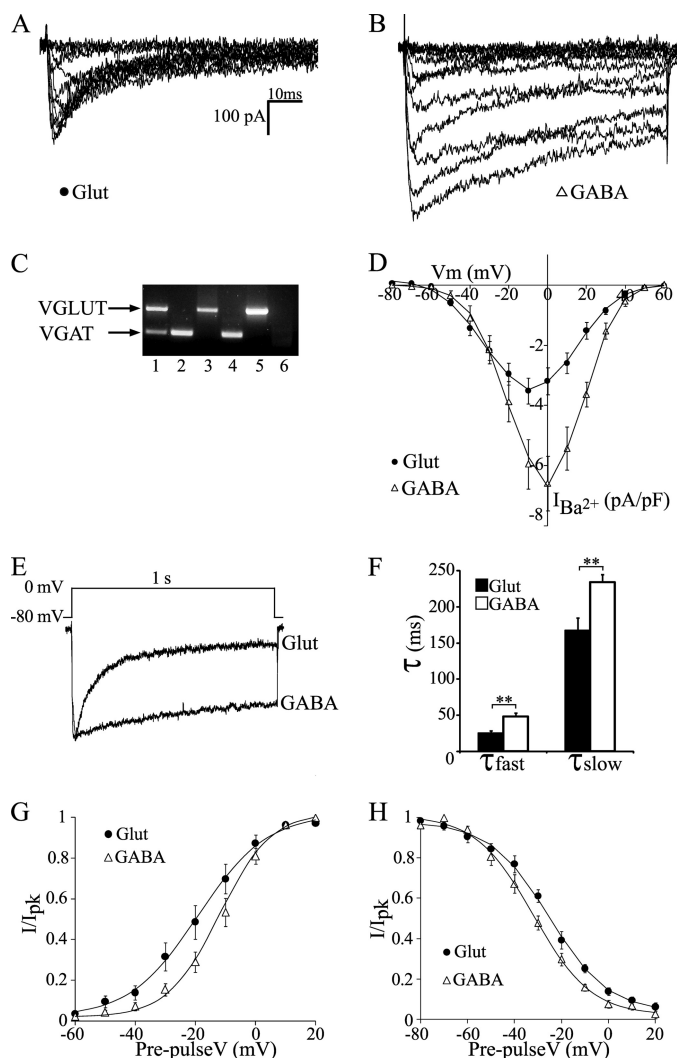


**FIGURE 1. Reduced VGCC current density in glutamatergic compared with GABAergic neurons.** *A* and *B*, representative whole cell VGCC inward  $\text{Ba}^{2+}$  currents ( $I_{\text{Ba}}$ ) in response to 10-mV increment step depolarizations from  $-80$  to  $60$  mV recorded from glutamatergic (*A*) and GABAergic (*B*) hippocampal neurons. *C*, ethidium bromide-stained gel of the PCR products from adult rat hippocampus (*lane 1*, positive control), recorded GABAergic neurons (*lanes 2 and 4*), recorded glutamatergic neurons (*lanes 3 and 5*), and a mock harvest (*lane 6*, negative control) amplified with primers specific for VGLUT and VGAT. *D*, mean  $I$ - $V$  relationships of peak  $I_{\text{Ba}}$  current density in glutamatergic ( $n = 11$ ) and GABAergic ( $n = 9$ ) neurons. *E*, representative current traces in response to a 1-s depolarization were normalized and aligned to compare the open-state inactivation of VGCC currents recorded from glutamatergic and GABAergic neurons. *F*, inactivation rate constants of VGCC currents in glutamatergic and GABAergic neurons evoked by the voltage protocol shown in *A*. Current traces were best fit with a double-exponential function where fast ( $\tau_{\text{fast}}$ ) and slow time constants ( $\tau_{\text{slow}}$ ) are represented as the mean  $\pm$  S.E. (error bars) of 9 experiments (\*\*,  $p \leq 0.01$ ). *G*, voltage-dependent activation curves of VGCC currents was elicited in glutamatergic ( $n = 8$ ) and GABAergic ( $n = 8$ ) neurons where tail currents generated by a repolarization to  $-40$  mV were measured, normalized to the largest tail current in the series, and plotted against the prepulse voltage. *H*, voltage dependence of steady-state inactivation of VGCCs in glutamatergic ( $n = 7$ ) and GABAergic ( $n = 8$ ) neurons. A 4-s prepulse to the indicated potential was followed by a 10-ms test pulse to 0 mV, where test pulse currents for each prepulse were normalized to the peak current of the series.

## RESULTS

**Distinct VGCC Properties in Glutamatergic versus GABAergic Neurons**—To characterize VGCC properties in glutamatergic and GABAergic neurons, we recorded whole cell  $\text{Ba}^{2+}$  currents

in cultured rat hippocampal neurons at 9–13 DIV. Fig. 1*A* shows a representative  $I$ - $V$  trace from a glutamatergic neuron, characterized by lower peak  $\text{Ba}^{2+}$  currents that inactivated rapidly compared with the larger, slower inactivating currents of GABAergic neurons (Fig. 1*B*). To confirm the recorded neurons glutamatergic or GABAergic nature, we performed single-cell RT-PCR, where glutamatergic neurons were identified by the presence of a band for VGLUT and GABAergic neurons by a reaction product for VGAT (Fig. 1*C*). Mean  $I$ - $V$  relations demonstrate that  $\text{Ba}^{2+}$  currents were significantly elevated in GABAergic neurons and peaked at a more depolarized potential compared with peak  $\text{Ba}^{2+}$  currents in glutamatergic neurons (Fig. 1*D*), suggesting differences in voltage-dependent gating between VGCC currents of glutamatergic and GABAergic neurons. This was confirmed by examining the inactivation properties of VGCC currents in both types of neurons. Inactivation rate kinetics were determined by a double-exponential fit of current decay in response to a 1-s depolarization step to 0 mV (Fig. 1*E*). VGCC current inactivated at a faster rate in glutamatergic neurons (Fig. 1*E*), with both rate components being significantly faster than those in GABAergic neurons (Fig. 1*F*). In addition to kinetic differences, the voltage dependence of activation and inactivation of VGCC current varied between glutamatergic and GABAergic neurons. Fig. 1*G* shows that the steady-state activation curve was shifted to more depolarized potentials in GABAergic relative to glutamatergic neurons. The voltage dependence of inactivation was also distinct, with total VGCC currents in glutamatergic neurons inactivating at more depolarized potentials relative to GABAergic neurons (Fig. 1*H*). Overall, these data indicate that VGCC properties differ markedly between glutamatergic and GABAergic neurons.

**Differential VGCC Subtype Expression in Glutamatergic and GABAergic Neurons**—The distinct VGCC properties in glutamatergic and GABAergic neurons could be due to differential VGCC subtype expression at the soma of excitatory and inhibitory neurons. To test this hypothesis, we performed immunocytochemical analysis of L-type and P/Q-type channel expression in GABAergic and glutamatergic neurons maintained in culture for 9–13 days. Fig. 2*A* demonstrates that both L- and P/Q-type channels can be detected at the somatodendritic level in both GABAergic and glutamatergic neurons. To isolate the proportions of the whole cell current composed of L-, P/Q-, and N-type channels, the effect of the specific VGCC blockers nifedipine,  $\omega$ -agatoxin-IVA, and  $\omega$ -conotoxin-GVIA were tested on glutamatergic and GABAergic neurons. Fig. 2*B* demonstrates the time course of blocker administration and the percentage of VGCC current inhibited by each specific blocker in a representative glutamatergic neuron. Peak  $I_{\text{Ba}}$  was measured in response to an  $I$ - $V$  protocol initiated at current plateau after administration of each blocker and expressed as a percentage of current blocked relative to initial control values. The results indicate that glutamatergic neurons at 9–13 DIV exhibit a relatively low proportion of L-type current but higher a higher proportion of N- and P/Q-type current (Fig. 2*D*). These observations are supported by previous results which show that, although P/Q- and N-type channels are highly concentrated at synaptic ter-

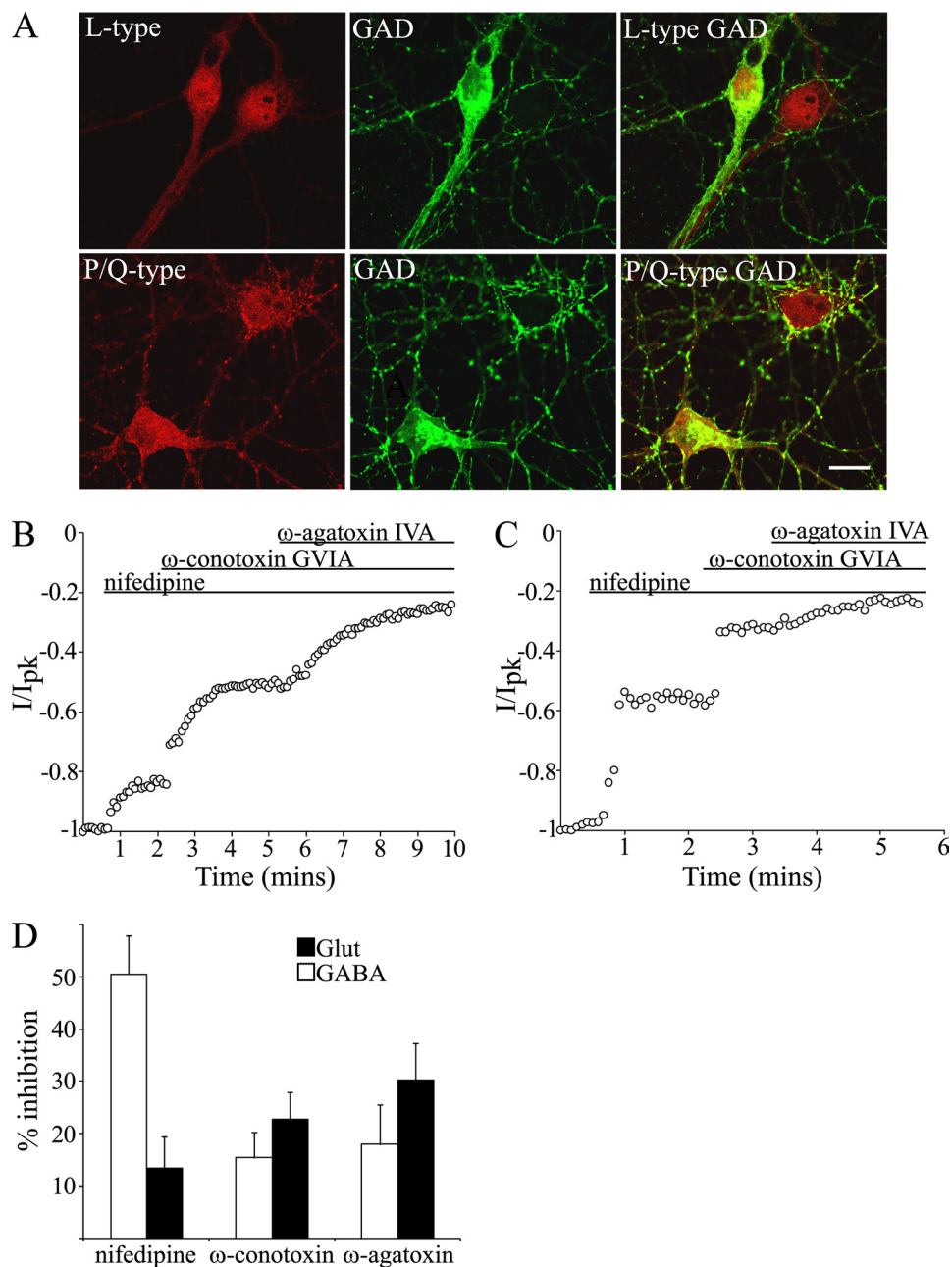


**FIGURE 2. Glutamatergic and GABAergic neurons exhibit a diverse sensitivity to specific VGCC subtype blockers.** *A*, immunocytochemical staining of neuronal cultures for L- and P/Q-type channels. GABAergic neurons are revealed by double labeling for glutamic acid decarboxylase (GAD, green). Scale bar, 10  $\mu$ m. *B* and *C*, representative traces of peak  $I_{Ba}$  versus time recorded from glutamatergic (*B*) and GABAergic (*C*) neurons during 50-ms depolarizations from a holding potential of  $-70$  mV to  $-10$  mV every 5 s with application of the specific VGCC blockers at the indicated times. *D*, inhibition of peak  $I_{Ba}$  by nifedipine (1  $\mu$ M),  $\omega$ -conotoxin-GVIA (1  $\mu$ M), or  $\omega$ -agatoxin-IVA (250 nM) in glutamatergic and GABAergic neurons expressed as the percentage of  $I_{Ba}$  inhibited after administration of each specific blocker ( $n = 6-11$ ). Error bars, S.E. of the mean.

minals, a somatodendritic localization of these channels has also been demonstrated by immunocytochemical (20, 22) and by electrophysiological (23) studies.

The percentage of VGCC current inhibited by the same blockers in a representative GABAergic neuron is shown in Fig. 2C. At an identical developmental stage *in vitro* (9–13 DIV), GABAergic neurons were characterized by a significant L-type current component with reduced fractions of N- and P/Q-type currents compared with glutamatergic neurons (Fig. 2D). This is in agreement with the predominant somatodendritic local-

ization of L-type channels detected by immunocytochemistry in cortical GABAergic neurons (24). Residual current in both cell types ( $\sim 20\%$ ) exhibited a variable sensitivity to the R-type channel blocker SNX (250 nM) but was reduced to zero with the general VGCC blocker cadmium (100  $\mu$ M) (data not shown). Overall, these data indicate that, at this stage in culture, the VGCC subtype profile differs markedly between glutamatergic and GABAergic neurons.

**Knockdown of Endogenous SNAP-25 in Glutamatergic Neurons Alters VGCC Properties**—It has been demonstrated previously that overexpression of SNAP-25 negatively modulates native VGCC function in neurons (8). To investigate whether endogenous SNAP-25 is physiologically involved in regulating native VGCC function, we measured VGCC properties in SNAP-25 silenced glutamatergic neurons. Knockdown of endogenous SNAP-25 by siRNA resulted in an increase in VGCC current density compared with scrambled siRNA or GFP transfected neurons (Fig. 3A). No significant difference in current density was observed between scrambled siRNA and GFP-transfected neurons (Fig. 3A). In addition, transfection of the scrambled siRNA had no significant effect on the voltage dependence of activation or inactivation relative to GFP transfected or nontransfected cells (data not shown). Taken together, these data indicate a specific effect of SNAP-25 knockdown on VGCC currents to reveal a physiological role for SNAP-25 in controlling glutamatergic VGCC function.

Because the total VGCC current is conducted by three main VGCC subtypes (Fig. 2C), we examined whether SNAP-25 silencing altered the relative subtype proportions in glutamatergic cells. However, the percentages of current sensitive to nifedipine,  $\omega$ -agatoxin-IVA, and  $\omega$ -conotoxin-GVIA, respectively, were not significantly different in SNAP-25-silenced glutamatergic neurons relative to wild type (Fig. 3B). These results suggest that endogenous SNAP-25 is able to modulate neuronal L-, N-, and P/Q-type currents equally and that in the absence of SNAP-25, current density increases due to a loss of negative regulation of available VGCC subtypes. Because P/Q-type channels dominate the VGCC conductance in glutamatergic neurons, we investigated

## Neuronal Calcium Channel Regulation by SNAP-25

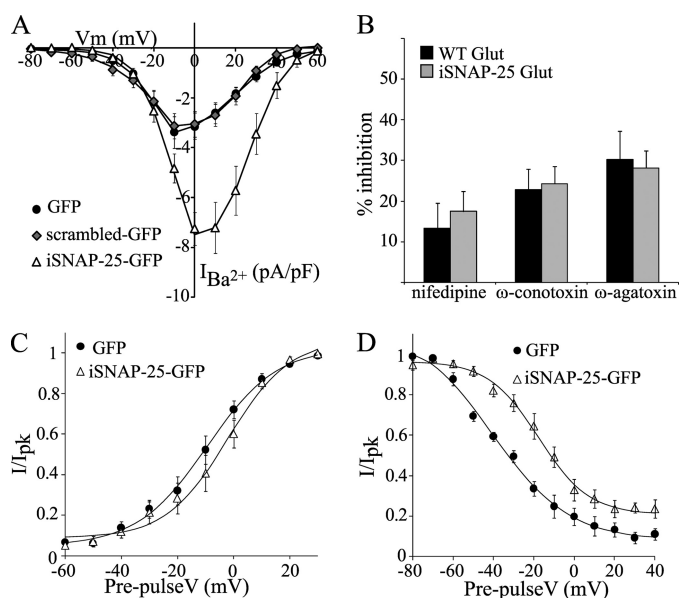


**FIGURE 3. Silencing of endogenous SNAP-25 in glutamatergic neurons augments VGCC properties.** *A*, mean  $I-V$  relationships of  $I_{Ba}$  current density in glutamatergic neurons co-transfected with pSuper SNAP-25 siRNA and GFP ( $n = 10$ ), pSuper scrambled siRNA and GFP ( $n = 8$ ), or GFP alone ( $n = 9$ ). *B*, inhibition of peak  $I_{Ba}$  by nifedipine ( $1 \mu\text{M}$ ),  $\omega$ -conotoxin-GVIA ( $1 \mu\text{M}$ ), or  $\omega$ -agatoxin-IVA ( $250 \text{ nM}$ ) in glutamatergic neurons co-transfected with iSNAP-25 and GFP or in nontransfected glutamatergic neurons. Data are expressed as the percentage of  $I_{Ba}$  inhibited after administration of each specific blocker ( $n = 6-12$ ). *C*, voltage dependence of steady-state activation of isolated P/Q-type current in glutamatergic neurons co-transfected with pSuper SNAP-25 and GFP ( $n = 8$ ) or GFP alone ( $n = 9$ ). *D*, voltage dependence of steady-state inactivation of isolated P/Q-type current in glutamatergic neurons co-transfected with pSuper SNAP-25 and GFP ( $n = 8$ ) or GFP alone ( $n = 9$ ). Error bars, S.E. of the mean.

how the silencing of SNAP-25 affected voltage-dependent activation and inactivation of pharmacologically isolated P/Q-type channels in glutamatergic neurons. Fig. 3C shows that silencing of SNAP-25 had no significant effect on the P/Q-type voltage dependence of activation. However, there was a pronounced depolarizing shift in the P/Q-type voltage dependence of inactivation associated with SNAP-25 silencing (Fig. 3D). Furthermore, under these conditions, a proportion of P/Q-type channel current failed to inactivate even at highly depolarized membrane potentials. These data indicate that in the absence of SNAP-25, VGCC current density could increase in glutamatergic neurons due to a reduced sensitivity to voltage-dependent inactivation of VGCCs implicating a direct effect of SNAP-25 on channel function.

**Localization of SNAP-25 and VGCCs in Glutamatergic and GABAergic Neurons**—Besides being localized at synapses, SNAP-25 is also expressed in nonsynaptic compartments, including the somatodendritic plasma membrane of cultured neurons (4, 13, 25). To evaluate whether SNAP-25 silencing generally affects VGCC expression and localization in cultured neurons, we performed immunofluorescence analysis of P/Q-type channels in glutamatergic neurons where SNAP-25 was knocked down by siRNA. SNAP-25 staining is reduced in iSNAP-25-transfected glutamatergic neurons (Fig. 4B). However, SNAP-25 silencing does not significantly affect syntaxin expression thereby indicating a specific effect of SNAP-25 knockdown (Fig. 4C). Analysis of P/Q-type channel localization showed no major alterations in channel distribution in the

soma of SNAP-25-silenced neurons (Fig. 4D). Furthermore, interfering with SNAP-25 expression did not affect P/Q-type channel sorting in neuronal processes (Fig. 4E) or in growth cones (Fig. 4F). These data indicate that reductions in VGCC current by SNAP-25 silencing are not a result of trafficking perturbations that reduce VGCC membrane expression or localization.

**Exogenous Expression of SNAP-25 in GABAergic Cells Negatively Regulates VGCC Properties**—Because endogenous SNAP-25 expression is lower in GABAergic compared with glutamatergic neurons (13, 26) we investigated whether SNAP-25-GFP overexpression in GABAergic neurons negatively modulates VGCC properties. Under these conditions, SNAP-25 is clearly detectable on the somatodendritic plasma membrane of GABAergic neurons (Fig. 5, A–D). In agreement with Verderio *et al.* (13), who observed a decrease in calcium dynamics in immunocytochemically positive GABAergic neurons overexpressing SNAP-25, peak  $Ba^{2+}$  currents were significantly reduced across a broad voltage range in SNAP-25-GFP-expressing GABAergic neurons compared with GFP-expressing controls (Fig. 5E). Interestingly, peak VGCC current density in SNAP-25-GFP GABAergic neurons ( $3.00 \pm 0.57 \text{ pA/pF}$ ) was reduced to similar levels recorded for GFP expressing glutamatergic neurons ( $3.38 \pm 0.63 \text{ pA/pF}$ ). This was associated with an increase in inactivation rates in GABAergic cells overexpressing SNAP-25-GFP (data not shown). To investigate whether SNAP-25-GFP overexpression altered the relative contributions of the three main VGCC subtypes, we analyzed the VGCC pharmacological profile in SNAP-25-GFP-transfected GABAergic neurons. Fig. 5F demonstrates that overexpression of SNAP-25-GFP did not significantly change the relative proportions of VGCC subtype-specific current compared with nontransfected GABAergic neurons. These results support the concept that VGCC properties vary with the extent of SNAP-25 expression as overexpression of SNAP-25 in GABAergic neurons shifts VGCC properties toward those of glutamatergic neurons.

**VGCC Properties in the SNAP-25 Heterozygous Mouse**—To provide further evidence that endogenous SNAP-25 plays a role in the regulation of VGCC in glutamatergic neurons, we measured VGCC current densities in hippocampal neuronal cultures isolated from wild type or *Snap-25*<sup>+/-</sup> mice. Fig. 6A shows that VGCC current densities in glutamatergic neurons from *Snap-25*<sup>+/-</sup> mice were significantly elevated compared with wild type glutamatergic neurons. These findings are in agreement with the increased calcium responsiveness observed in glutamatergic *Snap-25*<sup>+/-</sup> neurons (8) and suggest that reductions in endogenous SNAP-25 expression lead to enhanced VGCC activity.

In agreement with the experiments on rat neurons, VGCC current densities in wild type mouse GABAergic neurons were significantly greater than glutamatergic neurons (Fig. 6, A and B) but were similar between wild type and *Snap-25*<sup>+/-</sup> GABAergic neurons (Fig. 6B). Accordingly, no significant difference was detected in peak VGCC current density in SNAP-25-silenced rat GABAergic neurons ( $-5.60 \pm 0.74 \text{ pA/pF}$ ) compared with GFP-transfected ( $-5.54 \pm 0.63 \text{ pA/pF}$ ) controls. Although SNAP-25 expression was

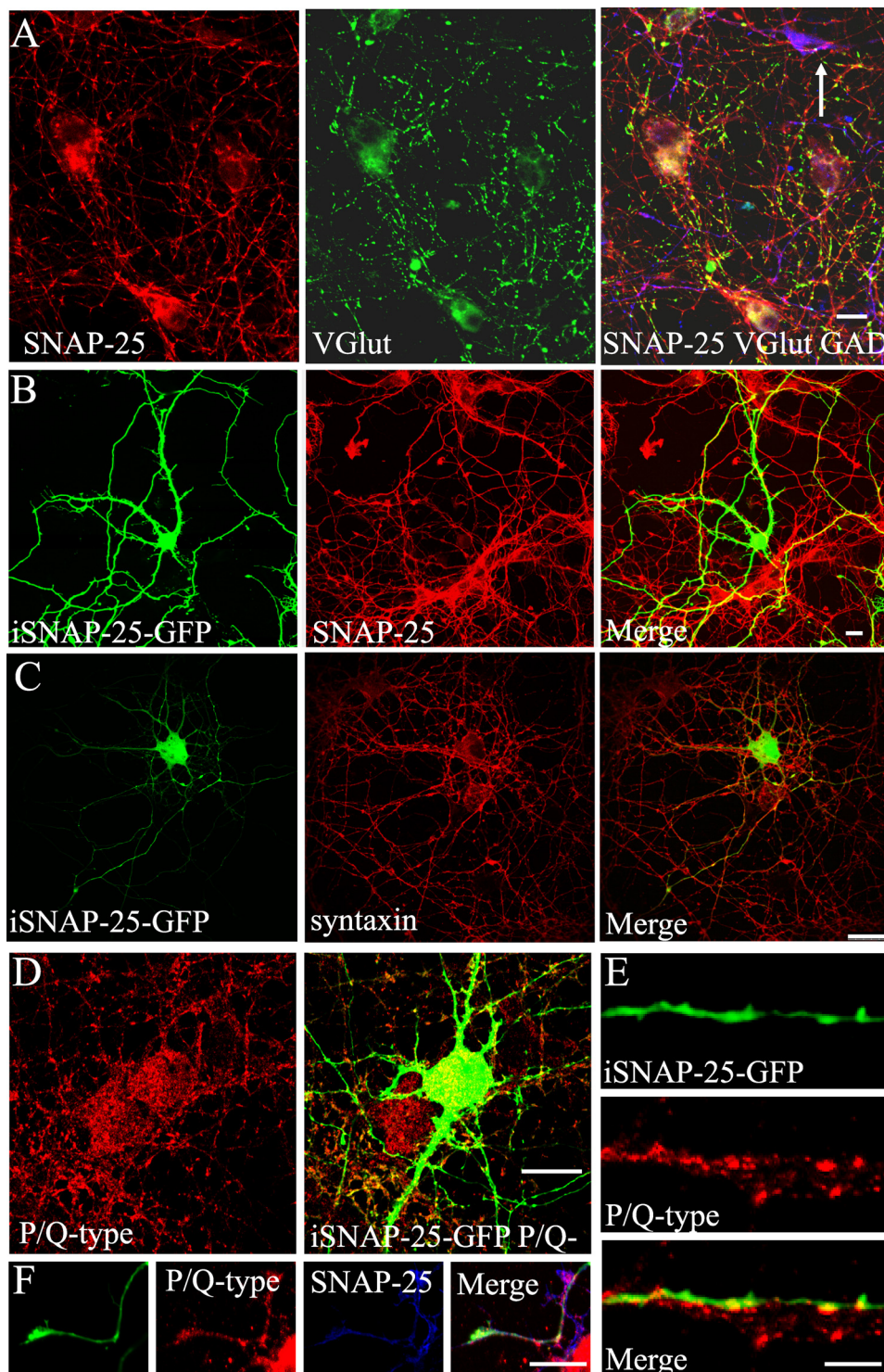


**FIGURE 4. Distribution of P/Q-type channels and syntaxin in SNAP-25-silenced neurons.** *A*, triple immunofluorescence labeling of hippocampal neurons for SNAP-25 (red), VGlut (green), and glutamic acid decarboxylase (GAD; blue). Arrow indicates a GAD-positive GABAergic neuron expressing lower levels of SNAP-25. *B* and *C*, hippocampal neurons co-transfected with iSNAP-25 and GFP and labeled for SNAP-25 (*B*) or syntaxin (*C*). Note the reduction of SNAP-25 expression (*B*) in the transfected cell whereas syntaxin expression (*C*) was not affected. *D–F*, labeling of iSNAP-25-GFP-transfected cultures for SNAP25 (green) and P/Q-type channels (red). Note that P/Q channels are expressed in the cell soma (*D*) and sorted in neurite varicosities (*E*) and growth cones (*F*) of both control and SNAP-25-silenced neurons. Neurons in *F* are triple-labeled for SNAP-25 (blue). Scale bars, 10  $\mu\text{m}$  (*A*, *B*, and *D*), 25  $\mu\text{m}$  (*C*), 7  $\mu\text{m}$  (*E*), and 3.5  $\mu\text{m}$  (*F*).

tantly, no difference in the expression of the  $\text{Ca}_v2.1$  P/Q-type channels or the  $\alpha2\delta2$  auxiliary subunit of VGCCs was detected in membrane fractions obtained from wild type or heterozygous mouse brains (Fig. 6D). These data indicate that reductions in SNAP-25 expression have less effect on VGCC properties in GABAergic neurons compared with glutamatergic neurons and support the evidence for a reduced functional role of SNAP-25 in controlling calcium dynamics in GABAergic neurons.

## DISCUSSION

The present study demonstrates that endogenous SNAP-25 negatively regulates native VGCC properties in glutamatergic neurons. Silencing of endogenous SNAP-25 in glutamatergic neurons lead to an augmentation of VGCC activity, slower inactivation kinetics, and a significant depolarizing shift in the voltage dependence of inactivation of the dominant P/Q-type current. Furthermore, VGCC current density was significantly increased in *Snap-25*<sup>+/-</sup> glutamatergic neurons relative to wild type. It is possible that the effects of reducing endogenous SNAP-25 expression may have a greater impact on VGCC regulation than on the function of the protein as a SNARE. This is supported by results where SNAP-25 knock-down by siRNA, which we have shown to impact on VGCC function heavily, does not alter SV exo-endocytotic recycling.<sup>4</sup> Similarly, genetic reductions in SNAP-25 expression do not impact on SNARE-dependent neurotransmission (27, 28). Therefore, reduced levels of SNAP-25 are sufficient to support exocytosis, but variations in SNAP-25 expression level alter VGCC function, which would impact on network excitability. This could have important consequences for pathologies in which expression of SNAP-25 is decreased, including schizophrenia and epilepsy (11, 29).

reduced in membrane fractions from *Snap-25*<sup>+/-</sup> mouse brains, there was no difference in syntaxin expression or expression of other membrane proteins (Fig. 6D). Impor-

<sup>4</sup> C. Verderio, unpublished observations.

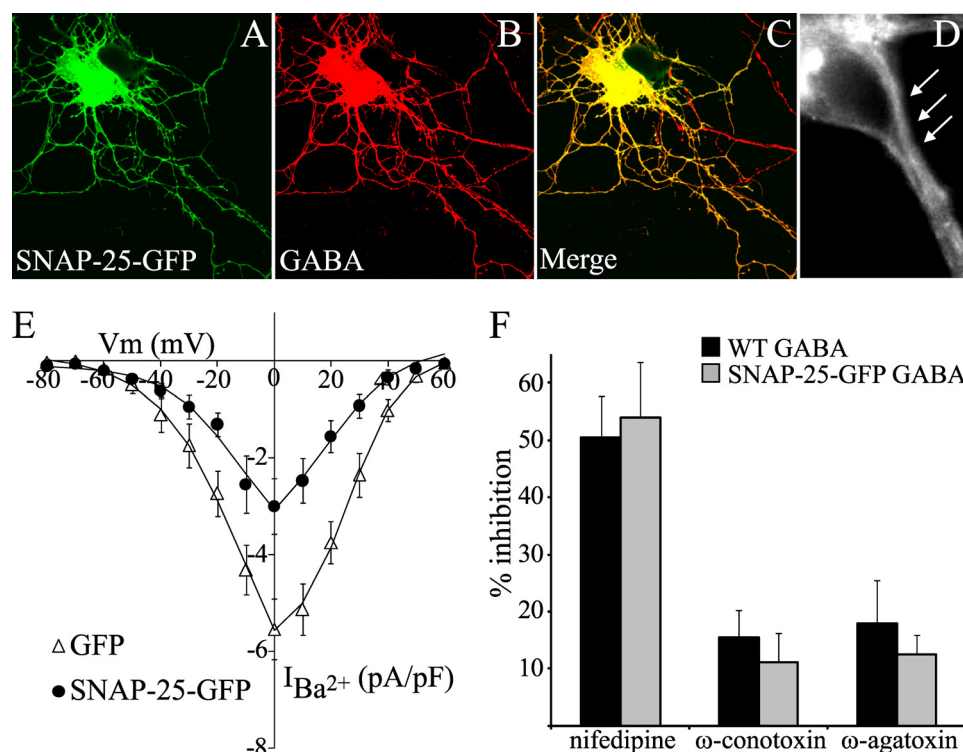


FIGURE 5. SNAP-25 exogenous expression in GABAergic neurons down-regulates VGCC function. A–D, immunolocalization of GABA in a SNAP-25-GFP-transfected neuron. Note the presence of SNAP-25 at the plasma membrane of the somatic region of transfected neurons (*inset*). E, mean *I*-*V* relationships of  $I_{Ba}$  current density in GABAergic neurons transfected with either GFP ( $n = 8$ ) or SNAP-25-GFP ( $n = 13$ ). F, inhibition of peak  $I_{Ba}$  by nifedipine ( $1 \mu\text{M}$ ),  $\omega$ -conotoxin-GVIA ( $1 \mu\text{M}$ ), or  $\omega$ -agatoxin-IVA ( $250 \text{ nM}$ ) in GABAergic neurons transfected with SNAP-25-GFP or in nontransfected GABAergic neurons. Data are expressed as the percentage of  $I_{Ba}$  inhibited after administration of each specific blocker ( $n = 6$ – $12$ ). WT, wild type.

SNAP-25 specifically binds to the  $\text{Ca}_v1$  (30),  $\text{Ca}_v2.1$  (31), and  $\text{Ca}_v2.2$  (32) pore-forming  $\alpha1$  subunits, leading to a variety of regulatory effects on VGCC function. In human embryonic kidney cells transfected with P/Q-type channels, co-expression of SNAP-25 negatively shifted the voltage dependence of inactivation which could be reversed with co-expression of syntaxin, synaptotagmin, and vesicle-associated membrane protein (7). Wisner *et al.* (30) demonstrated that SNAP-25 exerts differential effects on L- and N-type channels when co-expressed in *Xenopus* oocytes. SNAP-25 inhibited inward N-type currents and positively shifted the voltage dependence of inactivation without affecting the inactivation rate. In contrast, SNAP-25 inhibited L-type currents and increased the rate of inactivation without shifting the voltage dependence of inactivation.

In the present study, glutamatergic neurons were characterized by lower VGCC current densities, faster inactivation rates, and shifted voltage-dependent activation and inactivation curves relative to GABAergic neurons. One possible interpretation of these results is that these diverse VGCC properties are the consequence of differential levels of endogenous SNAP-25 physically interacting with somatodendritic VGCCs to alter channel function. This conclusion is supported by the fact that silencing of endogenous SNAP-25 in glutamatergic neurons increased VGCC properties toward GABAergic levels, whereas overexpressing SNAP-25 in GABAergic neurons reduced inward VGCC current and inactivation kinetics. Similar effects of reduced SNAP-25 expression on VGCCs in glutamatergic *Snap-25<sup>+/-</sup>* neurons further support this concept. Interest-

ingly, however, no significant difference in  $\text{Ca}^{2+}$  influx in response to depolarization was reported between wild type and *Snap-25<sup>-/-</sup>* neurons (33). These discrepancies could reflect the diverse experimental approaches where ratiometric measurements reflect total changes in the intracellular  $\text{Ca}^{2+}$  concentration, including contributions from  $\text{Ca}^{2+}$ -induced  $\text{Ca}^{2+}$  release from intracellular stores and, in the absence of specific antagonists, influx via ionotropic receptors. In contrast, whole cell  $\text{Ba}^{2+}$  currents measured in the present study reflect the specific activity of neuronal VGCCs. Meanwhile, although evidence against a trafficking mechanism is provided by our immunocytochemical and immunoblotting results, we cannot exclude that subtle differences in the trafficking of VGCC or regulatory subunits may contribute to the observed phenomenon.

The differences in VGCC properties observed in this study are likely to have important consequences for

neuronal function. Because we used the somatic voltage clamp, we cannot make conclusions about how a potentially diverse regulation of synaptic terminal VGCCs by SNAP-25 could influence inhibitory *versus* excitatory neurotransmission. Although SNAP-25 has been shown to be necessary for its role as a SNARE in mediating synaptic transmission at GABAergic terminals (34), it would be interesting to determine whether reduced expression of SNAP-25 could alter synaptic transmission via effects on presynaptic VGCC regulation. At the somatodendritic level, the absence of SNAP-25 negative regulation of VGCCs would be expected to increase GABAergic neuronal excitability relative to glutamatergic neurons. This could explain an increased basal intracellular calcium concentration (35), a more depolarized resting membrane potential (36), increased calcium responsiveness to depolarization (13, 35), and, because VGCCs play an important role in determining the generation and timing of action potential firing patterns (37, 38), could also contribute to the fast spike-firing phenotype of GABAergic neurons. Because enhanced excitability is essential in GABAergic neurons for generating rapid and temporally precise signaling for the normal operation of neuronal network activity (39), it is possible that the lack of negative regulation of GABAergic somatodendritic VGCCs by SNAP-25 contributes to an increased interneuron excitability. In contrast, decreased VGCC activity caused by negative regulation of SNAP-25 in excitatory glutamatergic neurons could contribute to restricting excitatory output to prevent excess excitation. Indeed, reductions in SNAP-25 expression have been correlated with

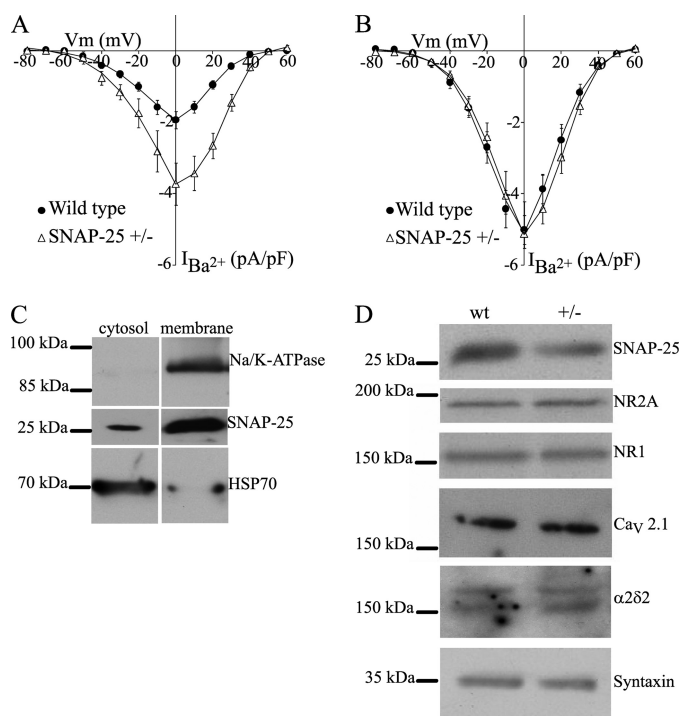


**FIGURE 6. VGCC properties in wild type and SNAP-25 heterozygous mouse neurons.** *A*, mean  $I$ - $V$  relationships of  $I_{Ba}$  current density in wild type ( $n = 12$ ) and  $Snap-25^{+/-}$  ( $n = 12$ ) glutamatergic neurons. *B*, mean  $I$ - $V$  relationships of  $I_{Ba}$  current density in wild type ( $n = 9$ ) and  $Snap-25^{+/-}$  ( $n = 9$ ) GABAergic neurons. *C*, enrichment of  $Na^{+}/K^{+}$ -ATPase and SNAP-25 in membrane fractions prepared from mouse brains. The heat shock protein Hsp70 is recovered mainly in the cytosolic fraction. *D*, membrane fractions prepared from heterozygous samples contain reduced levels of SNAP-25 but comparable levels of the NMDA receptor subunits NR1 and NR2A, and syntaxin relative to wild type (wt). Note the equivalent expression of the  $Ca_v2.1$  P/Q-type channels and the  $\alpha2\delta$  auxiliary subunit of VGCCs in wild type and heterozygous fractions.

neurological conditions characterized by increased network excitability. For example, VGCC currents are up-regulated resulting in absence-like epilepsy (29) and hyperactivity (40) in the *Coloboma* mouse mutant characterized by the heterozygous deletion of the SNAP-25 gene. Also, a missense mutation in *Snap-25* in the blind-drunk mutant mouse (41) results in impaired sensorimotor gating, anxiety, and apathy characteristic of a schizophrenic phenotype. Importantly, alterations in SNAP-25 expression have been described in human patients with attention deficit hyperactivity disorder (42) and schizophrenia (9).

Overall, our results demonstrate that endogenous SNAP-25 negatively regulates native VGCC properties in glutamatergic neurons. This regulation could play an important role in controlling normal neuronal network activity where perturbations in this regulation could lead to various neurological conditions.

**Acknowledgments**—We thank Dr. M. Wilson (University of New Mexico, Albuquerque, NM) for the SNAP-25 mutant mice; Dr. O. Rossetto (Dipartimento di Scienze Biomediche Sperimentali, Università di Padova) for the SNAP-25-GFP cDNA; and Drs. W. A. Catterall (University of Washington), M. Solimena (University of Dresden), and P. Rosa (Consiglio Nazionale delle Ricerche, Milano) for the antibodies. We are also grateful to Alice Giani and Silvia DeAstis (University of Milano, Italy) for help with some experiments and analysis.

## REFERENCES

- Südhof, T. C., and Rothman, J. E. (2009) *Science* **323**, 474–477
- Ji, J., Tsuk, S., Salapatek, A. M., Huang, X., Chikvashvili, D., Pasyk, E. A., Kang, Y., Sheu, L., Tsumishima, R., Diamant, N., Trimble, W. S., Lotan, I., and Gaisano, H. Y. (2002) *J. Biol. Chem.* **277**, 20195–20204
- Fan, H. P., Fan, F. J., Bao, L., and Pei, G. (2006) *J. Biol. Chem.* **281**, 28174–28184
- Selak, S., Paternain, A. V., Aller, M. I., Aller, I. M., Picó, E., Rivera, R., and Lerma, J. (2009) *Neuron* **63**, 357–371
- Catterall, W. A., and Few, A. P. (2008) *Neuron* **59**, 882–901
- Wiser, O., Bennett, M. K., and Atlas, D. (1996) *EMBO J.* **15**, 4100–4110
- Zhong, H., Yokoyama, C. T., Scheuer, T., and Catterall, W. A. (1999) *Nat. Neurosci.* **2**, 939–941
- Pozzi, D., Condliffe, S., Bozzi, Y., Chikhladze, M., Grumelli, C., Proux-Gillardeaux, V., Takahashi, M., Franceschetti, S., Verderio, C., and Matteoli, M. (2008) *Proc. Natl. Acad. Sci. U.S.A.* **105**, 323–328
- Thompson, P. M., Sower, A. C., and Perrone-Bizzozero, N. I. (1998) *Biol. Psychiatry* **43**, 239–243
- Young, C. E., Arima, K., Xie, J., Hu, L., Beach, T. G., Falkai, P., and Honer, W. G. (1998) *Cereb. Cortex* **8**, 261–268
- Thompson, P. M., Egbufoama, S., and Vawter, M. P. (2003) *Prog. Neuro-psychopharmacol. Biol. Psychiatry* **27**, 411–417
- Verderio, C., Bacci, A., Coco, S., Pravettoni, E., Fumagalli, G., and Matteoli, M. (1999) *Eur. J. Neurosci.* **11**, 2793–2800
- Verderio, C., Pozzi, D., Pravettoni, E., Inverardi, F., Schenk, U., Coco, S., Proux-Gillardeaux, V., Galli, T., Rossetto, O., Frassoni, C., and Matteoli, M. (2004) *Neuron* **41**, 599–610
- Sucher, N. J., and Deitcher, D. L. (1995) *Neuron* **14**, 1095–1100
- Huttner, W. B., Schiebler, W., Greengard, P., and De Camilli, P. (1983) *J. Cell Biol.* **96**, 1374–1388
- Taverna, E., Francolini, M., Jeromin, A., Hilfiker, S., Roder, J., and Rosa, P. (2002) *J. Cell Sci.* **115**, 3909–3922
- Verderio, C., Coco, S., Fumagalli, G., and Matteoli, M. (1994) *J. Cell Biol.* **126**, 1527–1536
- Taverna, E., Saba, E., Linetti, A., Longhi, R., Jeromin, A., Righi, M., Clementi, F., and Rosa, P. (2007) *J. Neurochem.* **100**, 664–677
- Hell, J. W., Westenbroek, R. E., Warner, C., Ahljanian, M. K., Prystay, W., Gilbert, M. M., Snutch, T. P., and Catterall, W. A. (1993) *J. Cell Biol.* **123**, 949–962
- Westenbroek, R. E., Sakurai, T., Elliott, E. M., Hell, J. W., Starr, T. V., Snutch, T. P., and Catterall, W. A. (1995) *J. Neurosci.* **15**, 6403–6418
- Pietrini, G., Matteoli, M., Banker, G., and Caplan, M. J. (1992) *Proc. Natl. Acad. Sci. U.S.A.* **89**, 8414–8418
- Westenbroek, R. E., Hell, J. W., Warner, C., Dubel, S. J., Snutch, T. P., and Catterall, W. A. (1992) *Neuron* **9**, 1099–1115
- Pravettoni, E., Bacci, A., Coco, S., Forbicini, P., Matteoli, M., and Verderio, C. (2000) *Dev. Biol.* **227**, 581–594
- Timmermann, D. B., Westenbroek, R. E., Schousboe, A., and Catterall, W. A. (2002) *J. Neurosci. Res.* **67**, 48–61
- Tao-Cheng, J. H., Du, J., and McBain, C. J. (2000) *J. Neurocytol.* **29**, 67–77
- Garbelli, R., Inverardi, F., Medici, V., Amadeo, A., Verderio, C., Matteoli, M., and Frassoni, C. (2008) *J. Comp. Neurol.* **506**, 373–386
- Bronk, P., Deák, F., Wilson, M. C., Liu, X., Südhof, T. C., and Kavalali, E. T. (2007) *J. Neurophysiol.* **98**, 794–806
- Delgado-Martínez, I., Nehring, R. B., and Sørensen, J. B. (2007) *J. Neurosci.* **27**, 9380–9391
- Zhang, Y., Vilaythong, A. P., Yoshor, D., and Noebels, J. L. (2004) *J. Neurosci.* **24**, 5239–5248
- Wiser, O., Trus, M., Hernández, A., Renström, E., Barg, S., Rorsman, P., and Atlas, D. (1999) *Proc. Natl. Acad. Sci. U.S.A.* **96**, 248–253
- Rettig, J., Sheng, Z. H., Kim, D. K., Hodson, C. D., Snutch, T. P., and Catterall, W. A. (1996) *Proc. Natl. Acad. Sci. U.S.A.* **93**, 7363–7368
- Sheng, Z. H., Rettig, J., Cook, T., and Catterall, W. A. (1996) *Nature* **379**, 451–454
- Tafoya, L. C., Shuttleworth, C. W., Yanagawa, Y., Obata, K., and Wilson, M. C. (2008) *BMC Neurosci.* **9**, 105



## Neuronal Calcium Channel Regulation by SNAP-25

34. Tafoya, L. C., Mameli, M., Miyashita, T., Guzowski, J. F., Valenzuela, C. F., and Wilson, M. C. (2006) *J. Neurosci.* **26**, 7826–7838
35. Grumelli, C., Berghuis, P., Pozzi, D., Caleo, M., Antonucci, F., Bonanno, G., Carmignoto, G., Dobszay, M. B., Harkany, T., Matteoli, M., and Verderio, C. (2008) *Mol. Cell. Neurosci.* **39**, 314–323
36. Mott, D. D., Turner, D. A., Okazaki, M. M., and Lewis, D. V. (1997) *J. Neurosci.* **17**, 3990–4005
37. Puopolo, M., Raviola, E., and Bean, B. P. (2007) *J. Neurosci.* **27**, 645–656
38. Bender, K. J., and Trussell, L. O. (2009) *Neuron* **61**, 259–271
39. Jonas, P., Bischofberger, J., Fricker, D., and Miles, R. (2004) *Trends Neurosci.* **27**, 30–40
40. Hess, E. J., Collins, K. A., and Wilson, M. C. (1996) *J. Neurosci.* **16**, 3104–3111
41. Jeans, A. F., Oliver, P. L., Johnson, R., Capogna, M., Vikman, J., Molnár, Z., Babbs, A., Partridge, C. J., Salehi, A., Bengtsson, M., Eliasson, L., Rorsman, P., and Davies, K. E. (2007) *Proc. Natl. Acad. Sci. U.S.A.* **104**, 2431–2436
42. Mill, J., Richards, S., Knight, J., Curran, S., Taylor, E., and Asherson, P. (2004) *Mol. Psychiatry* **9**, 801–810